

Giant magnetoresistance: Comparison of band-structure and interfacial-roughness contributions

T. N. Todorov, E. Yu. Tsymbal, and D. G. Pettifor

Department of Materials, University of Oxford, Parks Road, Oxford OX1 3PH, England, United Kingdom

(Received 19 June 1996)

A real-space Green-function technique, in which the scattering is treated exactly, is used in a single-band tight-binding model to evaluate the Ohmic resistivities and the giant magnetoresistance in trilayer systems. The model includes (i) spin dependence of the density of states and Fermi velocity in the magnetic material, giving a qualitative representation of Co/Cu and Fe/Cr systems; (ii) spin-independent bulk disorder, representing intrinsic defects in real systems; (iii) chemically sharp interfacial roughness. It is found that for parameters that produce realistic total resistivities, the spin-polarized band structure in conjunction with the spin-independent bulk disorder gives the main contribution to the giant magnetoresistance. The chemically sharp interfacial roughness enhances the effect. Its contribution becomes significant in the limit of sufficiently dense roughness steps, sufficiently weak bulk disorder, and sufficiently thin magnetic layers. [S0163-1829(96)50342-5]

Since the discovery of giant magnetoresistance (GMR) in magnetic multilayers,¹ the mechanism of the effect has been the subject of much discussion.² Spin-dependent scattering has, generally, been accepted as the origin of GMR. However, the spin dependence can arise both from the electronic band structure and from the actual scattering potentials. For example, spin-dependent scattering potentials can be produced by roughness at the interfaces between neighboring ferromagnetic and nonmagnetic layers, and can result in sizeable GMR.³⁻⁵ On the other hand, an accurate spin-dependent electronic structure, in conjunction with spin-independent bulk disorder, representing intrinsic defects in the multilayers, yields realistic GMR even for perfect interfaces.⁶

Here, we report calculations of GMR in trilayers, for the current-in-plane geometry, within a simple tight-binding model. The model includes three factors: spin-dependent band structure, spin-independent bulk disorder, and interfacial roughness. The band structure takes account of the difference in density of states (DOS) and Fermi velocity between the two spins in the magnetic material. The bulk disorder represents intrinsic structural defects in real systems and takes the form of a spin-independent random variation in the atomic on-site energies. The roughness takes the form of chemically sharp interfacial steps of random lengths. The aim of the calculations is to compare the contributions of the spin-dependent band structure and the interfacial roughness to the GMR effect.

The geometry for the calculations is shown in Fig. 1. The system consists of a single trilayer connected to two identical semi-infinite perfect leads. The trilayer consists of a nonmagnetic spacer layer of average thickness d_s , sandwiched between two ferromagnetic layers of average thickness d_m . The trilayer and the leads have a simple cubic geometry of lattice parameter a , and consist of rectangular (100) atomic layers stacked along the longitudinal [100] direction. The trilayer and the leads have the same cross section with a width w of eight atoms. The interfacial roughness steps along the trilayer have random lengths l_{step} . The configurational average of l_{step} defines the correlation length $l_{\text{cor}} = \langle l_{\text{step}} \rangle$ of the roughness. The height h_{step} of the steps is two atoms.

We use a single-band nearest-neighbor orthonormal tight-binding model with parameters chosen to give a qualitative representation of the electronic properties (DOS and velocity) of Co/Cu and Fe/Cr systems at the Fermi energy (E_F). It is known (e.g., Ref. 7) that in Co, E_F lies within the sp band for the majority spin electrons, and within the d band for the minority spin electrons. At E_F , the electronic properties of Cu are similar to those of the majority spins in Co. In the case of Fe, E_F lies within the d band for both spin orientations. However, Fe exhibits a pronounced valley in the DOS for the minority spins, with E_F lying near the bottom of this valley. The electronic properties of Cr are similar to those for the minority spins in Fe. Let the term “down-spin” stand for the minority spin in the case of Co/Cu and for the majority spin in the case of Fe/Cr. Let the term “up-spin” stand for the majority spin in Co/Cu and for the minority spin in Fe/Cr. Then, in each case, at E_F the down-spin in the magnetic material has a higher DOS than the up-spin, while the electronic properties of the spacer material are similar to those of the up-spin in the magnetic material.

Here, no attempt is made to calculate the full band structure of these materials. Instead, we aim to model qualitatively the above-described features at E_F only, treating the two spins as two decoupled systems. To this end, we have chosen the following parameters for the tight-binding model. The unperturbed (disorder-free) on-site energies for both spins are everywhere the same, and equal to zero. The hopping integral in the spacer layer and that for the up-spin in the magnetic layers are the same, and define the unit of energy. The hopping integral for the down-spin in the magnetic layers is set to 1/3. The hopping integral between nonequivalent species is taken as the geometric average of the respective “native” hopping integrals. E_F is set to -0.5 , slightly off the band center. The different hopping integrals, as opposed to simple rigid on-site energy shifts,^{4,5} provide the required difference in electronic properties between the two spins. In particular, at E_F , the bulk DOS for the down-spin in the magnetic material exceeds that for the up-spin and for the spacer material by a factor of 3 with a reciprocal difference in the Fermi velocities, giving a qualitative representation of real systems.

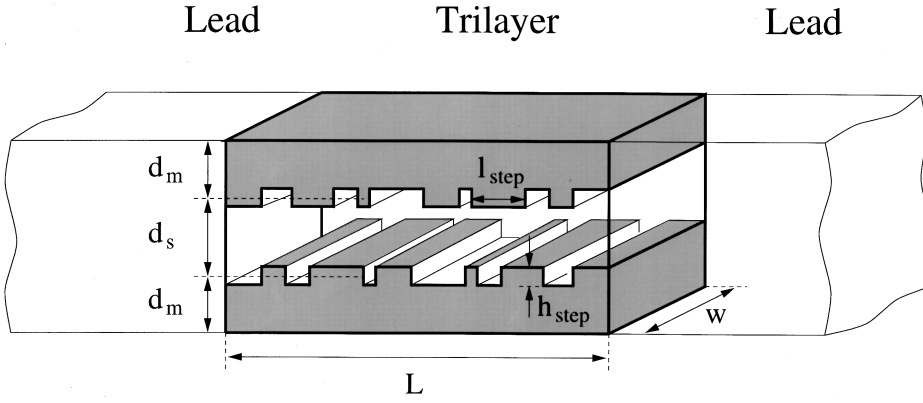


FIG. 1. The geometry used in the calculations. The details are explained in the main text.

Bulk disorder in the trilayer takes the form of a random variation of the on-site energies, with a uniform distribution with a mean of zero and a standard deviation of γ . The parameter γ is the same for both spins and on all atoms in the trilayer. This on-site disorder represents the spin-independent scattering potentials of intrinsic structural defects in real systems. The mean free path (MFP) and the bulk conductivity are roughly proportional to the square of the hopping integral and inversely proportional to γ^2 (Ref. 8). Thus, in our case, the MFP and the bulk conductivity for the up-spin exceed those for the down-spin in the magnetic material by a factor close to 10.

We use a real-space Green-function technique, in which the scattering of the electrons by the disorder is treated exactly, to evaluate the Ohmic resistivities for each spin in each magnetic configuration of the trilayer. Details about the method may be found elsewhere.^{8,9} The calculation starts with a standard growth sequence in which a trilayer of length L is grown, layer by layer, onto one lead, while the Green function on the last added layer is recalculated at each step by solving numerically the respective Dyson equation. After the trilayer has been fully grown, it is connected to the other lead (Fig. 1). The hopping integral and the on-site energy in the perfect leads are unity and zero, respectively. For a given spin, the zero-temperature conductance G , between imaginary equilibrium particle reservoirs at either extremity of the lead-trilayer-lead system, is found from^{8,9}

$$G = e^2 \pi \hbar \text{Tr}[d(E_F) I d(E_F) I]. \quad (1)$$

Here, $2\pi i d(E) = G^-(E) - G^+(E)$, where $G^\pm(E)$ are the retarded and advanced Green functions for the lead-trilayer-lead system, and I is the particle current operator between the trilayer and the right lead. If H is the full Hamiltonian, and $\{|r\rangle\}$ are all atomic basis states in the right lead, then $i\hbar I = [P, H]$, where $P = \sum_r |r\rangle\langle r|$.

The conductance is averaged over different realizations of the disorder, giving a resistance $R = 1/\langle G \rangle$ for the respective trilayer length L . The averaging is over 30 configurations per length. R includes additive contributions from the lead-reservoir contacts and from the trilayer-lead boundaries.⁸ These contributions will affect the value of GMR that would be obtained directly from R for a fixed L .⁴ To eliminate the effect of the contact resistances, here, the calculation is performed for a range of trilayer lengths, and the linear region of the R versus L relation is used to obtain the actual ohmic resistivity $\rho = A(dR/dL)$, where A is the trilayer cross sec-

tion. The range of L , from which ρ is calculated, typically exceeds the effective MFP in the trilayer by a factor between 5 and 10, so that we always are in the diffusive regime. The error in ρ arising from deviations from ohmic behavior due to localization effects, and from the statistical spread of the calculated conductances, is estimated as 2%.

The GMR effect is given by the ratio $\text{GMR} = (\rho_{AP} - \rho_P)/\rho_P$, where AP designates the configuration, in which the magnetizations of the ferromagnetic layers are antiparallel, and P designates the configuration in which these magnetizations are parallel. In each configuration, the conductivities for the two separate spins are taken to be additive. The *absolute* error in the GMR ratios is estimated as 3%.

Figure 2 shows the calculated GMR for different values of γ , without and with interfacial roughness of average step length l_{cor} of two atoms. The magnetic and spacer layer thicknesses d_m and d_s are set to four atoms each. GMR is nonzero even in the absence of the roughness. The effect arises from the difference in MFP and bulk resistivity between the up-spin and the down-spin in the magnetic material,¹⁰ which in turn comes from the respective difference in DOS and Fermi velocity. GMR increases with decreasing γ . In the limit of small γ , the MFP for both spins becomes much larger than the trilayer thickness, and GMR, in the absence of the roughness, reaches a saturation value. In the present case, this value is about 50%. In general, it

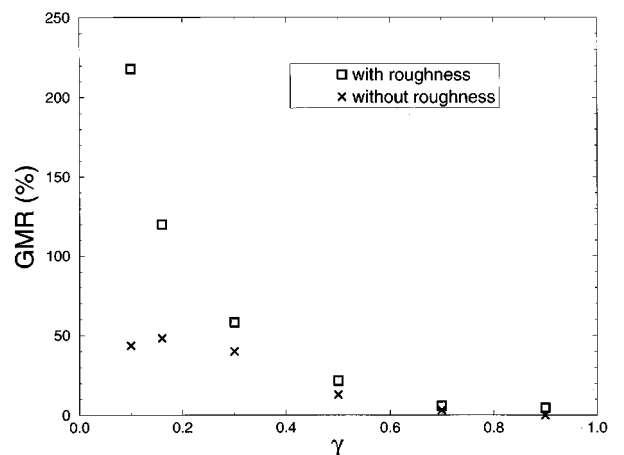


FIG. 2. GMR as a function of γ , the standard deviation of the random on-site energies, for the cases without and with interfacial roughness. l_{cor} is two atoms, and d_m and d_s are four atoms each.

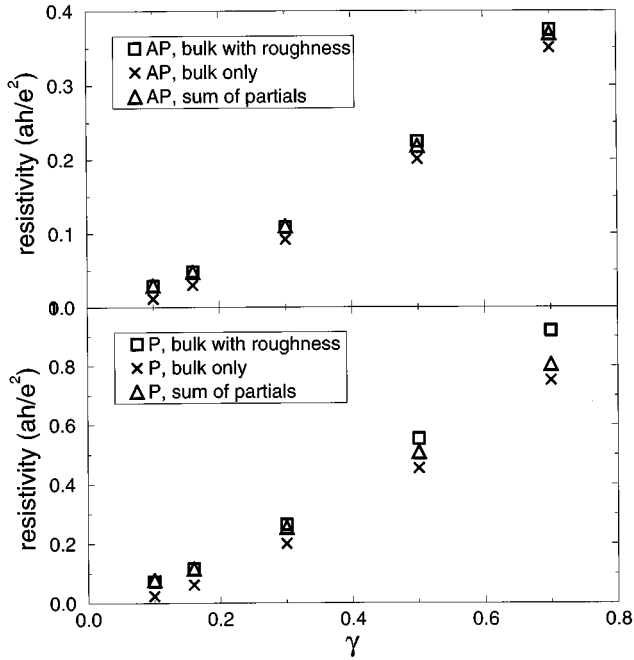


FIG. 3. Resistivity as a function of γ for the down-spin, in the *AP* (upper panel) and *P* (lower panel) configurations, for bulk scattering combined with interfacial roughness and for bulk scattering only, together with the sum of the partial resistivities for the two separate scattering mechanisms. l_{cor} is two atoms.

would depend on the particular band structure and on the ratio of the magnetic and spacer layer thicknesses. In the limit of large γ , the MFP for both spins becomes smaller than the trilayer thickness, and GMR approaches zero. The above results indicate that the spin-dependent band structure, in conjunction with the intrinsic bulk disorder in real systems, is a sufficient condition for GMR. This is consistent with results for the ballistic regime¹¹ and for the semiclassical Boltzmann regime.¹²

As may be seen from Fig. 2, the roughness enhances GMR. However, the contribution of the roughness becomes dominant only in the limit of small γ . To define the regime in which the roughness is important, we have calculated the resistivity for the down-spin in the *AP* and *P* configurations, as a function of γ , for the cases of bulk scattering only, interfacial scattering only, and bulk scattering combined with interfacial scattering. The results are presented in Fig. 3. The partial resistivities due to the two separate scattering mechanisms effectively add in series over a range of γ . Deviations become apparent for large γ , with the resistivity for the combined disorder exceeding the sum of partials, as may be expected from Matthiessen's inequality.¹³ Comparison of Figs. 2 and 3 suggests that the contribution of the roughness to GMR becomes dominant when the contribution of the roughness to the resistivity becomes dominant. In our case, this happens for $\gamma < 0.2$.

In the present model, GMR with the roughness included tends to infinity when $\gamma \rightarrow 0$. The reason is that as the hopping integrals for the up-spin in the *P* configuration are everywhere the same, this spin sees no difference between the layers and has zero resistivity in the limit $\gamma \rightarrow 0$, giving $\rho_P = 0$ with infinite GMR. In reality, there will be some up-

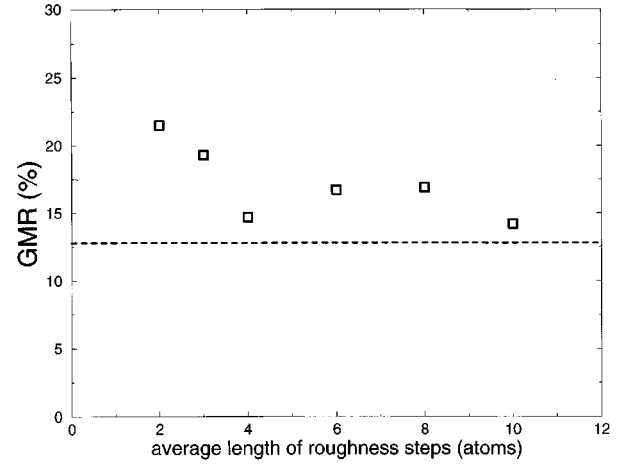


FIG. 4. GMR as a function of the average length of the roughness steps, for the case $\gamma = 0.5$, with d_m and d_s equal to four atoms each. The dashed line gives the GMR value without the roughness.

per bound on the effect. In general, ignoring bulk disorder and having interfacial roughness as the only scattering mechanism, with accurate band structure can lead to unrealistically high GMR.¹⁴

In the rest of the calculations, the parameter γ is set equal to 0.5. With d_m and d_s equal to four atoms each, and with $a = 0.2$ nm, this yields a total saturation resistivity (in the *P* configuration), for the case without roughness, of about $45 \mu\Omega$ cm, which is a representative value for real systems.¹ Figure 4 shows GMR as a function of the correlation length of the roughness, with d_m and d_s equal to four atoms each. As l_{cor} increases, GMR decreases, approaching its value for the case without the roughness. The oscillations are probably due to calculational error. Figure 4 can be understood in terms of the earlier discussion: as l_{cor} increases, the partial resistivity of the roughness (which is proportional to the rate of roughness scattering per unit trilayer length) decreases, and so does the contribution of the roughness to GMR.

Finally, we examine the dependence of GMR on the thickness of the layers. Figure 5 shows GMR, without and with roughness, as a function of spacer layer thickness d_s .

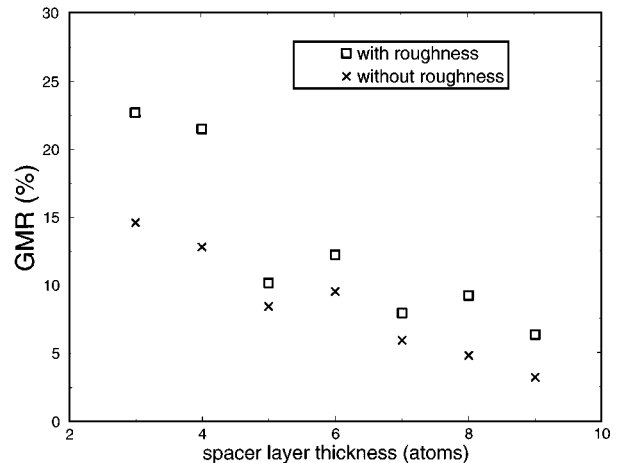


FIG. 5. GMR, without and with roughness, as a function of spacer layer thickness, for fixed magnetic layer thickness of four atoms. l_{cor} is two atoms and $\gamma = 0.5$.

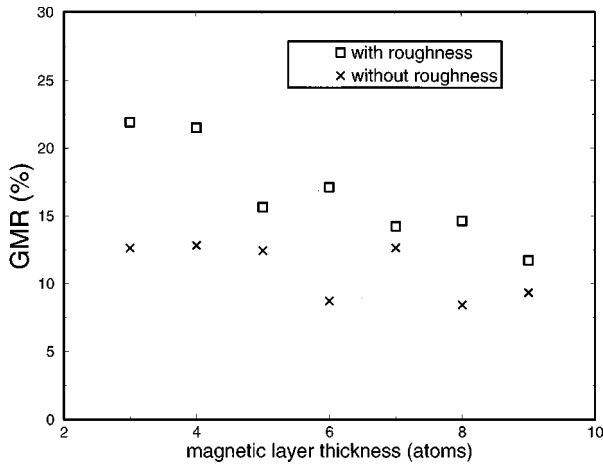


FIG. 6. GMR, without and with roughness, as a function of magnetic layer thickness, for fixed spacer layer thickness of four atoms. l_{cor} is two atoms and $\gamma=0.5$.

As may be expected, GMR decreases with increasing d_s . The oscillations may in part be due to calculational error, and in part to quantum finite-size effects. GMR without and with the roughness decrease at approximately the same rate, so that the fractional contribution of the roughness remains approximately constant. The dependence of GMR on the magnetic layer thickness d_m is different. As may be seen from Fig. 6, GMR decreases with increasing d_m , but in the case with the roughness, the decrease is faster than in the case without the roughness. This may be understood as follows. The partial contribution of the roughness to GMR decreases approximately as $1/d_m$, as the roughness scattering is confined to the interfaces. The contribution of the bulk disorder to GMR, on the other hand, decreases as $1/d_m$ only in the limit when d_m exceeds greatly the MFP for the up-spin, which in this case is estimated as $14a$. In fact, this contribu-

tion is expected to go through a maximum¹⁰ when d_m is of the order of the MFP for the down-spin in the magnetic layer, which in this case is estimated as $1.5a$. We are, therefore, just beyond this maximum, with a slow initial decrease of GMR in the case without the roughness. Thus, for the roughness to have a significant effect against this steady background, it is necessary to have thin magnetic layers.

For the roughness to produce the spin-dependent scattering potentials, considered in this paper, it is essential to have chemically sharp interfaces, so that the ferromagnetic material retains its magnetic properties at the interfaces. Then, as has been demonstrated experimentally,¹⁵ dense roughness steps in high quality Fe/Cr multilayers with magnetic layer thickness of a few monolayers can result in large GMR. Interdiffusion or alloying at the interfaces, on the other hand, can result in a paramagnetic interfacial layer with spin-independent disorder, and reduces GMR.¹⁶

In conclusion, we have used a Green-function technique, in which the scattering is treated exactly, to evaluate the ohmic resistivities and the GMR effect in trilayer systems. We find that the spin-polarized band structure, in combination with the spin-independent bulk disorder, is sufficient for the occurrence of GMR, and for parameters, producing realistic total resistivities, these two factors give the dominant contribution to the effect. The chemically sharp interfacial roughness generally enhances the effect. The contribution of the roughness, however, becomes quantitatively significant only in the limit of sufficiently dense interfacial steps (small correlation length of the roughness), sufficiently weak bulk scattering, and sufficiently thin magnetic layers.

The calculations for this paper were carried out at the Materials Modelling Laboratory at Oxford University, which is partially funded by the EPSRC under Grant No. GR/H/58278. E.Yu.T. is grateful to Hewlett-Packard Laboratories in Palo-Alto for financial support. T.N.T. is grateful to St. John's College, Oxford, for financial support.

¹M. N. Baibich, J. M. Broto, A. Fert, F. Nguyen Van Dau, F. Petroff, P. Etienne, G. Creuzet, A. Friederich, and J. Chazelas, Phys. Rev. Lett. **61**, 2472 (1988).

²A. Fert and P. Bruno, in *Ultrathin Magnetic Structures II*, edited by B. Heinrich and J. A. C. Bland (Springer, Berlin, 1994).

³P. M. Levy, S. Zhang, and A. Fert, Phys. Rev. Lett. **65**, 1643 (1990).

⁴Y. Asano, A. Oguri, and S. Maejawa, Phys. Rev. B **48**, 6192 (1993).

⁵H. Itoh, J. Inoue, and S. Maekawa, Phys. Rev. B **51**, 342 (1995).

⁶E. Yu. Tsympal and D. G. Pettifor, J. Phys. Condens. Matter **8**, L569 (1996).

⁷D. A. Papaconstantopoulos, *Handbook of the Band Structure of Elemental Solids* (Plenum, New York, 1986).

⁸T. N. Todorov, Phys. Rev. B **54**, 5801 (1996).

⁹P. A. Lee and D. S. Fisher, Phys. Rev. Lett. **47**, 882 (1981).

¹⁰D. M. Edwards, in *Electron Theory in Alloy Design*, edited by D. G. Pettifor and A. H. Cottrell (Institute of Materials, London, 1992), Chap. 9.

¹¹K. M. Schep, P. J. Kelly, and G. E. W. Bauer, Phys. Rev. Lett. **74**, 586 (1995).

¹²P. Zahn, I. Mertig, M. Richter, and H. Eschrig, Phys. Rev. Lett. **75**, 2996 (1995).

¹³N. W. Ashcroft and N. D. Mermin, *Solid State Physics* (Saunders College, Philadelphia, 1976), Chap. 16.

¹⁴R. K. Nesbet, J. Phys. Condens. Matter **6**, L449 (1994).

¹⁵R. Schad, C. D. Potter, P. Beliën, G. Verbanck, J. Dekoster, G. Langouche, V. V. Moshchalkov, and Y. Bruynseraede, J. Magn. Mater. **148**, 331 (1995).

¹⁶M. Suzuki and Y. Taga, Phys. Rev. B **52**, 361 (1995).